

UNSUPERVISED SINGLE IMAGE UNDERWATER DEPTH ESTIMATION

Honey Gupta, Kaushik Mitra

Computational Imaging Lab, Indian Institute of Technology Madras, India

ABSTRACT

Depth estimation from a single underwater image is one of the most challenging problems and is highly ill-posed. Due to the absence of large generalized underwater depth datasets and the difficulty in obtaining ground truth depth-maps, supervised learning techniques such as direct depth regression cannot be used. In this paper, we propose an unsupervised method for depth estimation from a single underwater image taken “in the wild” by using haze as a cue for depth. Our approach is based on indirect depth-map estimation where we learn the mapping functions between unpaired RGB-D terrestrial images and arbitrary underwater images to estimate the required depth-map. We propose a method which is based on the principles of cycle-consistent learning and uses dense-block based auto-encoders as generator networks. We evaluate and compare our method both quantitatively and qualitatively on various underwater images with diverse attenuation and scattering conditions and show that our method produces state-of-the-art results for unsupervised depth estimation from a single underwater image.

Index Terms— underwater depth, unsupervised, depth estimation, deep learning

1. INTRODUCTION

Exploration and mapping of underwater regions has always been a topic of interest. With the advancement in technology, it is now possible to visually explore the deep underwater regions that were unseen by humans few years back (like Mariana Trench). One of the most interesting fields of underwater exploration and mapping is 3D reconstruction, a key aspect of which is depth or 3D point estimation of the underwater scenes.

The current approaches for depth estimation of underwater regions either rely on specialized hardware sensors like time-of-flight (ToF)[1] and structured light[2] or use image processing methods to estimate the depth map from a single or a set of images. Stereo based techniques[3, 4] have also been used but they require feature matching, for which the images have to be enhanced first. This, in itself, is a challenging problem.

Single underwater image depth estimation approaches [5, 6, 7, 8, 9] mainly focus on image restoration. They estimate the transmission-map as an intermediate step and derive depth-maps and restored images from that. Transmission-map is related to the depth-map and scattering parameter via an exponential relationship $t(x) = e^{-\beta d(x)}$. Recovering the depth-map from the transmission-map implicitly assumes a specific scattering parameter, which might be incorrect. These approaches produce good results but due to the possibility of multiple depth-maps from a single transmission-map, a better approach would be to directly estimate depth from the underwater image.

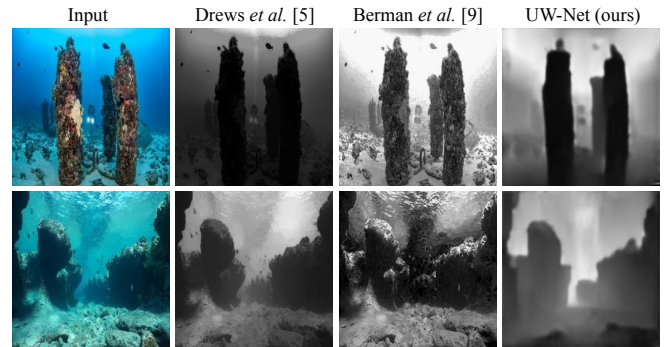


Fig. 1: Instead of following the usual approach of obtaining depth-map from transmission-map, we propose a novel depth estimation network based on unsupervised learning. Columns 2-3 show results from transmission-map based methods; column 4 shows our results.

Recently, deep learning based techniques have shown great promise for estimating depth from a single above-water image. Supervised approaches such as the methods proposed in [10] or [11] use large above-water datasets to train deep neural networks. Unsupervised methods like [12] use stereo dataset for training. However, these approaches are not suitable for estimating depth from underwater images due to the unavailability of large datasets consisting of underwater (stereo) images and their corresponding ground truth depth-maps. To tackle this issue, we propose an unsupervised approach of transferring style between underwater and hazy above-water RGB-D images.

In both underwater and hazy above-water images, the physical factors behind haze-like effect are different but the visual effects are similar i.e. visibility decreases as depth increases. The appearance of an underwater photo is governed by light scattering and attenuation as it propagates through water. This results in a depth-dependent function that relates the albedo of underwater objects to a hazy appearance from the camera’s point of view. We aim to exploit this similarity between underwater and above-water hazy appearances to learn depth-map estimation.

We take a generative approach of style-transfer and use haze as a cue to learn the mapping functions between hazy underwater and hazy above-water color image and depth-map. Our proposed network consists of two circularly connected dense-block [13] based auto-encoders which learn to estimate depth-map from a single underwater image based on the principle of cycle-consistent learning [14]. Ideally, the transformed images should have the original structure of the source image and the desired style from the target image, but just having adversarial loss does not ensure that the original content and object structure of the images are preserved. To address this issue, we use SSIM [15] as a structural loss along with the adversarial loss for training the network. We also include a gradient sparsity loss term for the generated depth-map to reduce texture leakage arti-

facts in the depth-map. To summarize, the main contributions of this paper are as follows:

- We propose an unsupervised deep-learning based method for estimating depth-map from a single underwater image.
- We propose a network that contains circularly connected dense-block based auto-encoders that use structural and gradient sparsity loss to learn the mappings between hazy underwater and above-water hazy color image and depth-map.
- We demonstrate that the proposed depth estimation method produces state-of-the-art results by comparing it with other unsupervised methods both quantitatively and qualitatively.

2. PRIOR WORK

2.1. Underwater depth estimation

Active underwater depth estimation methods have been proposed in the past few years like the ones by Maccarone *et al.*[1] and Bruno *et al.*[2]. The article by Campos *et al.* [16] gives an overview of different sensors and methods that have been used for underwater 3D. For single image depth estimation, the dark channel prior (DCP) [17] was one of the first methods to be used. Many variations of DCP have been introduced for underwater depth estimation and de-hazing [5, 18, 6]. Emberton *et al.* [8] segment regions of pure veiling-light and adapt the transmission-map to avoid artifacts. Peng *et al.* [7] estimate the scene distance via image blurriness. Berman *et al.* [9] take into account multiple spectral profiles of different water types and choose the best result based on color distribution. Many of these methods focus on transmission-map estimation and obtain depth based on the relation between transmission-map and depth-map. Due to unknown scattering parameter and multiple possible solutions, these depth-map estimates are most likely to be incorrect.

2.2. Depth estimation from single image

Depth estimation approaches for single above-water images can be categorized as supervised and unsupervised methods. A variety of deep learning based supervised methods have been proposed, mostly comprising of training a model to predict depth from color image [10, 11, 19]. Other supervised techniques include joint estimation of depth with other related problems such as visual odometry [20]. Unsupervised methods for depth estimation include using stereo image pairs and photometric warp loss in place of reconstruction loss. Godard *et al.* [12] adopted this approach and used photometric loss between the warped left image and the right image. These unsupervised methods require large stereo datasets such as KITTI for training and are unsuitable for underwater scenario.

3. UNDERWATER DEPTH ESTIMATION NETWORK: (UW-NET)

In our proposed method, we learn to transform images from a domain of hazy underwater images X to a domain of hazy terrestrial RGB-D images Y and vice versa. The network learns the mapping between these domains with the help of unpaired images belonging to both the image distributions $x \sim p_{uw}(x)$ and $y \sim p_{aerial}(y)$. The network consists of two generator auto-encoder networks which learn the two mapping functions $G : X \rightarrow Y$ and $F : Y \rightarrow X$. It also consists of two discriminators D_X and D_Y . The generator and the discriminator learn through adversarial learning [21]. The discriminator D_X tries to classify its input as real ($\{x\}$) or fake

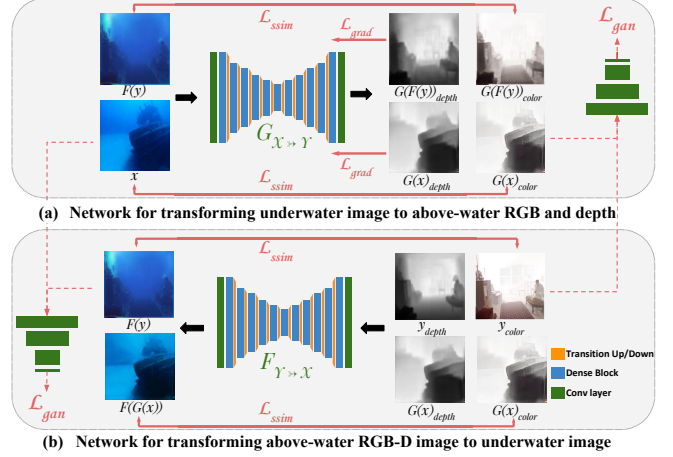


Fig. 2: Diagram representing the proposed UW-Net. Generator G transforms underwater images to above-water color and depth images whereas F converts above-water color and depth to underwater color image. G is constrained to learn depth estimation from underwater image due to the \mathcal{L}_{cyc} between above-water y and $G(F(y))$, thus producing depth-map from real underwater images.

($\{F(y)\}$) underwater image. The discriminator D_Y similarly classifies above-water images as real or fake. The generators' objective function is a weighted combination of four loss terms:

$$\mathcal{L}_{total}(G, F, D_X, D_Y) = \mathcal{L}_{cyc} + \gamma_{gan} \mathcal{L}_{gan} + \gamma_{ssim} \mathcal{L}_{ssim} + \gamma_{grad} \mathcal{L}_{grad} \quad (1)$$

The first two terms are cyclic \mathcal{L}_{cyc} and adversarial loss \mathcal{L}_{gan} , similar to CycleGAN[14]. We use \mathcal{L}_1 for \mathcal{L}_{cyc} loss and since the convergence of least squares version of \mathcal{L}_{gan} is better as compared to the log-likelihood loss [22], we use the least squares version of \mathcal{L}_{gan} .

$$\mathcal{L}_{gan}(G, D_Y, X, Y) = \mathbf{E}_{y \sim p_{aerial}(y)} [(D_Y(y) - 1)^2] + \mathbf{E}_{x \sim p_{uw}(x)} [D_Y(G(x))^2] \quad (2)$$

Adversarial loss is the only loss term that influences the image quality of the generated image after half a cycle in the CycleGAN[14] method, which does not guarantee preservation of structural properties of the input image in the transformed image. In order to alleviate this problem, we introduce structural similarity loss \mathcal{L}_{ssim} in the objective function. It is defined as $1 - SSIM(\cdot, \cdot)$ calculated between $\{x, G(x)\}$, $\{y, F(y)\}$, $\{G(x), F(G(x))\}$ and $\{F(y), G(F(y))\}$. In case of y , $G(x)$ and $G(F(y))$, we consider only the RGB channels, as including \mathcal{L}_{ssim} for depth introduces unwanted artifacts. In our training dataset, above-water RGB-D images belong to indoor scenes and this creates a mismatch between the geometry of objects in the above-water and underwater images. Due to this undesired textures get introduced in the estimated depth-maps. We introduce a sparsity of gradient loss \mathcal{L}_{grad} to reduce this texture. It is defined as

$$\mathcal{L}_{grad} = \sum (\|\nabla_x d\|_1 + \|\nabla_y d\|_1) \quad (3)$$

where d is the depth channel of $G(x)$.

Network architecture. Fig.2 depicts a schematic diagram of our network architecture. We use a dense-block based auto-encoder network [23] for the generator. It consists of 5 dense blocks (DB)

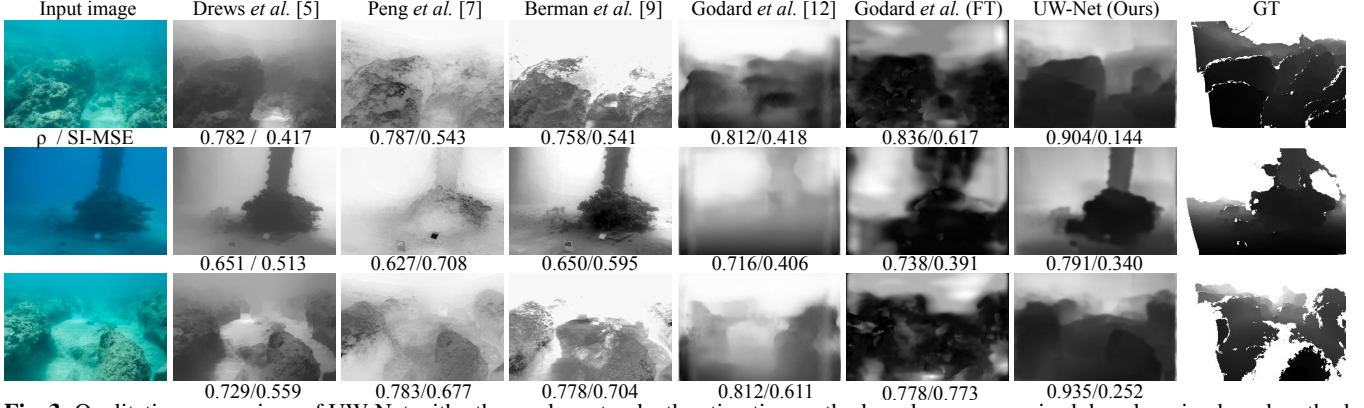


Fig. 3: Qualitative comparison of UW-Net with other underwater depth estimation methods and an unsupervised deep learning based method (Godard *et al.* [12]) on few images from Berman *et al.*’s [9] dataset. Our method produces meaningful depth-maps and has the highest Pearson coefficient and lowest scale-invariant error for the shown images. For further discussion on qualitative analysis, please refer to section 4.2.2.

| | DCP | Drewe et al.[5] | Berman et al.[9] | Peng et al. [7] | Godard et al. [12] | Godard et al. (FT) | UW-Net (Ours) |
|---------------------|-------|-----------------|------------------|-----------------|--------------------|--------------------|---------------|
| $\rho \uparrow$ | 0.086 | 0.556 | 0.669 | 0.722 | 0.803 | 0.732 | 0.828 |
| SI-MSE \downarrow | 2.022 | 0.450 | 0.518 | 0.485 | 0.311 | 0.363 | 0.221 |

Table 1: Quantitative comparison of our method with state-of-the-art algorithms on Berman *et al.*’s [9] dataset. The values were averaged over all the images. Higher ρ values and lower SI-MSE values are better.

+ transition down/up modules, where each DB has 5 layers with 16 filters. For discriminator, we use 70x70 PatchGANs, similar to [14].

Our proposed method is based on indirect learning of the depth map. An above-water image sample, $y \in Y$, is a four-channel data sample $y = [y_{color}, y_{depth}]$, where the fourth channel is the depth map. The output of our generator G is color as well as depth and so is the input of generator F . The discriminator D_Y also takes both color and depth images as input. We observed that including depth in discriminator D_Y helps the network produce better depth-maps. The discriminator D_X takes only color images as input. A 4-channel image y is passed through F to convert it to an underwater image. The obtained underwater image $F(y)$ is passed through G to obtain $G(F(y))$, which completes one cycle. Similarly, we transform $x \in X \rightarrow G(x) \rightarrow F(G(x))$, which forms another cycle. D_X enforces $F(y)$ to be close to underwater image-set X . Due to cyclic loss and “realness” of fake underwater image, the network G learns to estimate depth from single underwater image.

4. EXPERIMENTS

4.1. Training details

For our experiments¹, we collected 1343 real underwater images from different sources on the internet. We focused on collecting underwater images with different illumination and scattering conditions. For hazy above-water images, we have used the D-Hazy dataset [24]. The dataset consists of 1449 synthetic hazy indoor images. To reduce sensor noise in the ground truth depth-maps, we performed bilateral filtering on the depth images before training. All the images were down-sampled to a size of 256×256 and trained on random 128×128 patches for 400 epochs using ADAM optimizer, with a learning rate of 1×10^{-4} . While testing, we took complete images of size 256×256 . The experiments were performed on Nvidia GTX 1080Ti, using TensorFlow framework. We experimented with

the weights for each of the loss term and found the optimum values for γ_{gan} , γ_{ssim} and γ_{grad} to be 5, 1 and 1 respectively.

4.2. Comparison with other methods

We compare our depth estimation method with other underwater depth estimation methods by Drewe *et al.* (UDCP) [5], Peng *et al.* [7] and Berman *et al.* [9]. We also compare with a deep learning based depth estimation method by Godard *et al.* [12] which uses stereo image pairs and photometric warp loss for training. We used the codes publicly released by Drewe *et al.*, Berman *et al.* and Godard *et al.* for evaluation. For Peng *et al.*, we used the code provided by the authors. Default hyper-parameters were used for all the methods during evaluation. For all the transmission-map based methods, we took negative-log to obtain the depth map. For Godard *et al.* [12], we show two results, one with their pre-trained KITTI model and the other with a fine-tuned (FT) underwater model (Godard *et al.* (FT)). For the fine-tuned model, we re-trained the KITTI model for 20 epochs on 2000 stereo pairs randomly picked from three different subsets of CADDY dataset [25]. We fine-tuned our trained model for 20 epochs on Berman *et al.*’s dataset for better results.

4.2.1. Quantitative analysis

For the quantitative comparison, we have used the dataset released by Berman *et al.* [9]. It contains 114 underwater RGB images collected from 4 different locations along with the ground-truth depth-map (GT). We have used 98 images belonging to regions: Katzaa, Nachsholim and Satil. We did not use images from the region Michmoret as they have very less natural objects. Only pixels with a defined depth-value in GT were used for calculation. Since ours as well as all other methods produce depth-maps up to scale, we use two scale-invariant metrics for comparison: log Scale-Invariant Mean Squared Error (SI-MSE), as proposed by Eigen *et al.* in [10] and Pearson correlation coefficient (ρ) defined as $\rho_{X,Y} = \frac{cov(X,Y)}{\sigma_X \sigma_Y}$.

Table 1 shows the quantitative results. We observe that our method performs better than others and produces the highest Pearson coefficient and the least scale-invariant error. The closest to our

¹Please refer our project page: <http://bit.ly/uw-net> for code and results.

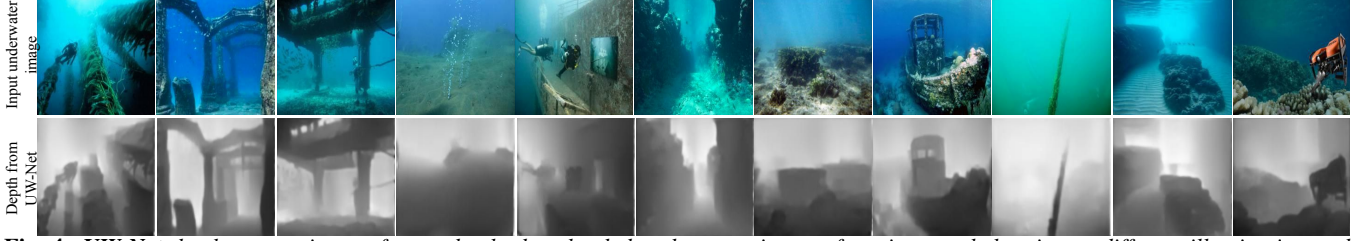


Fig. 4: UW-Net depth-map estimates for randomly downloaded underwater images from internet belonging to different illumination and scattering conditions. Comparison with other methods can be found at <https://goo.gl/tB22gU>.

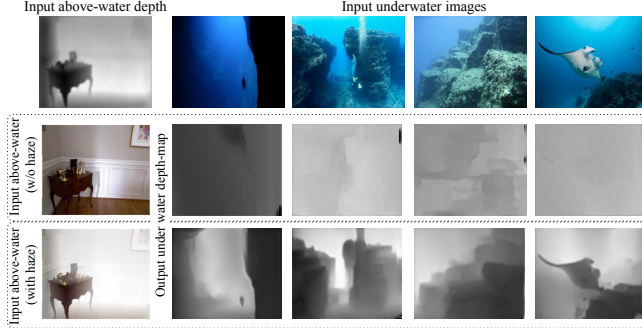


Fig. 5: With clear RGB above-water images during training, the network fails to learn the mapping between underwater image and the depth-map (row 2) but with hazy above-water images, the network is able to learn the mapping quite well (row 3).

approach is the pre-trained Godard *et al.* model, as it might be a somewhat generalized model. We think that fine-tuning reduces the accuracy as it over-fits the model for specific underwater conditions and hence fails for images belonging to other regions. Among other underwater depth-estimation methods, Peng *et al.* perform the best.

4.2.2. Qualitative analysis

Fig.3 depicts a comparison of our results with other methods for few single underwater images taken from Berman *et al.*'s dataset. Results for collected underwater images from internet with different illumination and scattering conditions can be found in Fig.1, Fig.4 and at this link: <https://goo.gl/ASJv2f>.

In Fig.3, column 1 shows the input underwater images, columns 2, 3 and 4 show the depth from image-processing based methods and columns 5 and 6 show results by Godard *et al.* w/o and with fine-tuning. In columns 2-4, a closer look at the sea-floor area near to the camera reveals that these methods fail to capture relative depth of the scene with respect to the camera. Moreover, there is excessive texture leakage in the estimated depth-maps as these methods mainly capture the transmission properties of the scene. For Godard *et al.*, we see improper results due to the mismatch between the train-test data samples. Even for the fine-tuned model, the results worsen as the images belong to different underwater regions. Due to unavailability of a diverse stereo dataset, stereo based methods are bound to perform moderately. On the other hand, our depth-maps seem much more reasonable with a linear depth variation and have higher ρ and lower scale-invariant error. Even for varying illumination, we observe that our network successfully captures the depth information.

| | EDSR | Hourglass | U-Net | ResNet | DenseRes | DenseNet |
|---------------------|-------|-----------|-------|--------|----------|--------------|
| $\rho \uparrow$ | 0.732 | 0.758 | 0.769 | 0.773 | 0.768 | 0.829 |
| SI-MSE \downarrow | 0.364 | 0.310 | 0.279 | 0.297 | 0.271 | 0.221 |

Table 2: Quantitative comparison of different auto-encoder networks as generator network on Berman *et al.*'s [9] dataset.

4.3. Ablation Study

4.3.1. Depth from clean vs. hazy RGB-D

Here we show the importance of using hazy above-water images during training and validate that our network learns to capture depth by using haze as a cue. We trained a separate network with the same configuration as UW-Net, but in place of D-Hazy dataset, we used the original NYU dataset (without haze). In Fig.5 row 2, we observe that the network using clear above-water images produces poor underwater depth-map estimates, whereas in row 3, UW-Net produces quite good depth-maps. We think this is because of the simpler relation between depth and haze as compared to depth and object geometry. Moreover, using hazy above-water images gives rise to depth-dependent attenuation in the transformed $F(y)$, which in turn helps G to learn the relation between depth and attenuation.

4.3.2. Choice of Generator Network

We experimented with different auto-encoder networks to find the best network architecture for the generator. The originally proposed Cycle-GAN [14] has ResNet [26] based generator network, which performs quite well. Table 2 shows the Pearson coefficient and scale-invariant error of the results obtained by training our network with U-Net [27], EDSR(w/o upsampling) [28], Hourglass [29], ResNet [26], FC-DenseNet56 [23] followed by 3 residual blocks (DenseRes) and DenseNet [23] models. Please refer to the referenced papers for further details regarding the networks. It can be seen from Table 2 that DenseNet produces the least scale-invariant error and the highest Pearson correlation coefficient, making it the best choice. Closest to DenseNet are ResNet [26] and DenseRes architectures.

5. CONCLUSION

We proposed an unsupervised method that uses haze as a cue to estimate depth-map from a single underwater image. Our method is based on cycle-consistent learning and uses dense-block based auto-encoder for generator networks. The proposed network learns indirectly to estimate the depth-map and uses SSIM and gradient sparsity loss for better estimation. We compared our method with existing state-of-the-art single image underwater depth estimation methods and showed that our method performs better than all other methods both qualitatively and quantitatively.

6. REFERENCES

- [1] A. Maccarone, A. McCarthy, X. Ren, R. E. Warburton, A. M. Wallace, J. Moffat, Y. Petillot, and G. S. Buller, "Underwater depth imaging using time-correlated single-photon counting," *Opt. Express*, vol. 23, no. 26, pp. 33911–33926, Dec 2015.
- [2] F. Bruno, G. Bianco, M. Muzzupappa, S. Barone, and A.V. Razionale, "Experimentation of structured light and stereo vision for underwater 3d reconstruction," *ISPRS Journal of Photogrammetry and Remote Sensing*, vol. 66, no. 4, pp. 508 – 518, 2011.
- [3] Y. Wu, R. Nian, and B. He, "3d reconstruction model of underwater environment in stereo vision system," in *Oceans-San Diego, 2013*. IEEE, 2013, pp. 1–4.
- [4] C. Sánchez-Ferreira, J. Y. Mori, M. CQ Farias, and C. H. Llanos, "A real-time stereo vision system for distance measurement and underwater image restoration," *Journal of the Brazilian Society of Mechanical Sciences and Engineering*, vol. 38, no. 7, pp. 2039–2049, 2016.
- [5] P. L.J. Drews, E. R. Nascimento, S. SC Botelho, and M. F. M. Campos, "Underwater depth estimation and image restoration based on single images," *IEEE computer graphics and applications*, vol. 36, no. 2, pp. 24–35, 2016.
- [6] C. O. Ancuti, C. Ancuti, C. De Vleeschouwer, L. Neumann, and R. Garcia, "Color transfer for underwater dehazing and depth estimation," in *Image Processing (ICIP), 2017 IEEE International Conference on*. IEEE, 2017, pp. 695–699.
- [7] Y. Peng, X. Zhao, and P. C. Cosman, "Single underwater image enhancement using depth estimation based on blurriness," in *Image Processing (ICIP), 2015 IEEE International Conference on*. IEEE, 2015, pp. 4952–4956.
- [8] S. Emberton, L. Chittka, and A. Cavallaro, "Underwater image and video dehazing with pure haze region segmentation," *Computer Vision and Image Understanding*, vol. 168, pp. 145–156, 2018.
- [9] D. Berman, D. Levy, T. Treibitz, and S. Avidan, "Underwater single image color restoration using haze-lines and a new quantitative dataset," 2018.
- [10] D. Eigen, C. Puhrsch, and R. Fergus, "Depth map prediction from a single image using a multi-scale deep network," in *Advances in neural information processing systems*, 2014, pp. 2366–2374.
- [11] A. Kendall, H. Martirosyan, S. Dasgupta, P. Henry, R. Kennedy, A. Bachrach, and A. Bry, "End-to-end learning of geometry and context for deep stereo regression," .
- [12] C. Godard, O. Mac Aodha, and G. J. Brostow, "Unsupervised monocular depth estimation with left-right consistency," in *CVPR*, 2017, vol. 2, p. 7.
- [13] G. Huang, Z. Liu, L. Van Der Maaten, and K. Q. Weinberger, "Densely connected convolutional networks," in *2017 IEEE Conference on Computer Vision and Pattern Recognition (CVPR)*. IEEE, 2017, pp. 2261–2269.
- [14] J. Zhu, T. Park, P. Isola, and A. A. Efros, "Unpaired image-to-image translation using cycle-consistent adversarial networks," in *Computer Vision (ICCV), 2017 IEEE International Conference on*, 2017.
- [15] Zhou Wang, Alan C Bovik, Hamid R Sheikh, and Eero P Simoncelli, "Image quality assessment: from error visibility to structural similarity," *IEEE transactions on image processing*, vol. 13, no. 4, pp. 600–612, 2004.
- [16] M. Massot-Campos and G. Oliver-Codina, "Optical sensors and methods for underwater 3d reconstruction," *Sensors*, vol. 15, no. 12, pp. 31525–31557, 2015.
- [17] K. He, J. Sun, and X. Tang, "Single image haze removal using dark channel prior," *IEEE transactions on pattern analysis and machine intelligence*, vol. 33, no. 12, pp. 2341–2353, 2011.
- [18] A. Galdran, D. Pardo, A. Picón, and A. Alvarez-Gila, "Automatic red-channel underwater image restoration," *Journal of Visual Communication and Image Representation*, vol. 26, pp. 132–145, 2015.
- [19] Z. Li and N. Snavely, "Megadepth: Learning single-view depth prediction from internet photos," in *Proceedings of the IEEE Conference on Computer Vision and Pattern Recognition*, 2018, pp. 2041–2050.
- [20] B. Ummenhofer, H. Zhou, J. Uhrig, N. Mayer, E. Ilg, Alexey Dosovitskiy, and Thomas Brox, "Demon: Depth and motion network for learning monocular stereo," in *IEEE Conference on computer vision and pattern recognition (CVPR)*, 2017, vol. 5, p. 6.
- [21] I. Goodfellow, J. Pouget-Abadie, M. Mirza, B. Xu, D. Warde-Farley, S. Ozair, A. Courville, and Y. Bengio, "Generative adversarial nets," in *Advances in neural information processing systems*, 2014, pp. 2672–2680.
- [22] X. Mao, Q. Li, H. Xie, R. Y. K. Lau, and Z. Wang, "Multi-class generative adversarial networks with the L2 loss function," *CoRR*, vol. abs/1611.04076, 2016.
- [23] S. Jégou, M. Drozdal, D. Vazquez, A. Romero, and Y. Bengio, "The one hundred layers tiramisu: Fully convolutional densenets for semantic segmentation," in *Computer Vision and Pattern Recognition Workshops (CVPRW), 2017 IEEE Conference on*. IEEE, 2017, pp. 1175–1183.
- [24] C. De Vleeschouwer C. Ancuti, C. O. Ancuti, "D-hazy: A dataset to evaluate quantitatively dehazing algorithms," in *IEEE International Conference on Image Processing (ICIP)*, 2016, ICIP'16.
- [25] A. G. Chavez, A. R., D. Chiarella, E. Zereik, A. Babic, and A. Birk, "Caddy underwater stereo-vision dataset for human-robot interaction (hri) in the context of diver activities," *CoRR*, vol. abs/1807.04856, 2018.
- [26] K. He, X. Zhang, S. Ren, and J. Sun, "Deep residual learning for image recognition," in *Proceedings of the IEEE conference on computer vision and pattern recognition*, 2016, pp. 770–778.
- [27] O. Ronneberger, P. Fischer, and T. Brox, "U-net: Convolutional networks for biomedical image segmentation," in *International Conference on Medical image computing and computer-assisted intervention*. Springer, 2015, pp. 234–241.
- [28] B. Lim, S. Son, H. Kim, S. Nah, and K. M. Lee, "Enhanced deep residual networks for single image super-resolution," in *The IEEE Conference on Computer Vision and Pattern Recognition (CVPR) Workshops*, July 2017.
- [29] W. Chen, Z. Fu, D. Yang, and J. Deng, "Single-image depth perception in the wild," in *Advances in Neural Information Processing Systems*, 2016, pp. 730–738.